Proceeding of the 2013 RSI/ISM International Conference on Robotics and Mechatronics
February 13-15, 2013, Tehran, Iran

Dynamics and Control of a Novel 3-DoF Spatial Parallel Robot

Mohsen Asgari
Dept. of Electrical and Computer Eng.
Qazvin Branch, Islamic Azad University
Qazvin, Iran
m.asgari@qiau.ac.ir

Mahdi Alinaghizadeh Ardestani
Dept. of Electrical & Computer Eng.
Qom University of Technology
Qom, Iran
ardestani@qut.ac.ir

Mersad Asgari
Faculty of Engineering and Technology
Imam Khomeini International University
Qazvin, Iran
mersad.asgari70@gmail.com

***Abstract*—Dynamics modeling and trajectory tracking control of a new structure of spatial parallel robots from Delta robots family is elaborated. The proposed novel mechanism like ordinary Delta parallel mechanism has three degrees of pure translational freedom, but the position of robot's three active joints relative to each other is the main difference between this mechanism and Delta parallel mechanism, which has caused the change in geometry of platforms, and it shapes the asymmetrical structure in the robot mechanism and its workspace. The inverse dynamic modeling is performed based on the principle of virtual work. This paper extends our previous paper in which we compared implementation of computed torque (C-T) method using adaptive neuro-fuzzy controller and conventional PD controller. The PD and PID controllers of C-T method usually need manual retuning to make a successful industrial application, particularly in the presence of disturbance. In the present paper, we study feasibility of applying fuzzy PD and PID supervisory control for PD and PID used in C-T method for this parallel mechanism. The main motivation for this design was to cope with above problem for this complex nonlinear system. Numerous computer simulations demonstrate the effectiveness of the proposed control method in comparison with ordinary C-T method.**

***Key words*—Robot Control, Parallel Manipulators, Dynamic Modeling, Fuzzy PID.**

I. INTRODUCTION

In the past three decades, parallel robots have attracted more and more researchers' attention, mainly due to their inherent advantages. A parallel manipulator is closed-loop mechanical structures generally composed of two platforms, which are connected by joints and legs acting in parallel. The last few years have witnessed an important development in the use of these robots in the industrial [1] and medical applications [2] because of their flexibility.

Dynamical analysis of the parallel manipulators is much more complicated than the serial manipulators because of the existence of multiple close-loop chains. A lot of interesting parallel manipulators dynamics with specified type and mechanical design methods has been extensively studied. General solution for the dynamic modeling of parallel robots has been presented in [3]. Staicu et al. have been proposed a novel dynamic modeling approach for parallel mechanisms analysis using recursive matrix relations in [4-6]. Kinematics and inverse dynamics analysis for a general 3-PRS spatial parallel mechanism have been performed in [7].

So far, the C-T method that has been implemented with PD and PID controller is one of the leading controllers in robotic systems. But, above-mentioned controller's performance is restricted. It is not necessary to discard these controllers which work well. It makes more sense to enhance their performance by appropriate choice of the PID gains. As a one trend, supervisory control can be used in order to improvements in conventional PD and PID controllers.

Fuzzy control system has been used as a supervisor to codify the human skills to re-tuning the PID gains, while the plant is in operation [8-12]. In [13], Kazemian tuned PID controller parameters by a fuzzy system. Fuzzy PID controller presents good performance for controlling general nonlinear systems [14, 15]. Also, it has been shown in [16, 17], that application of this controller enhances the closed loop performance of a PID controller for handling change in an operating point in complex nonlinear systems. Various linear and nonlinear systems have been tuned in [16, 17] and [18] with a fuzzy gain tuning inferencing mechanism. As well as, feasibility of applying adaptive neuro-fuzzy controller in C-T control method for parallel manipulator has been investigated in [19]. In [20, 21] the optimal parameters of fuzzy PD and PID have been obtained via reinforcement learning methods. Stability analysis of a fuzzy PID controller has been performed in [22, 23].

In this contribution, dynamic modeling and computed-torque control of a new structure of spatial parallel manipulators by employing a modified version of DELTA parallel manipulator are presented. For various applications, change in position of DELTA robot's three active joints relative to each other shapes this new asymmetrical structure with an optimal architecture rather than ordinary DELTA robot. The C-T control method has been implemented with diverse methods, first by applying conventional PD and PID controllers, then by utilizing the concept of supervisory control as another trend. The fuzzy supervisory control presented very interesting tracking features in both without disturbance conditions and in the presence of disturbance. The obtained simulation results from fuzzy gain scheduling controller are encouraging when compared with conventional controllers.

978-1-4673-5811-8/13/$31.00 ©2013 IEEE

This paper is organized as follows. In section 2, the architecture of the manipulator is described in details, after that, closed-form equations are developed for inverse kinematics and then velocity analysis is performed by generation of Jacobian matrix. Section3 describe the dynamic model of parallel mechanism based upon the principle of virtual work. The appropriate control methodology is implemented for exploited dynamic model in section 4. Section 5 represents the simulation results and finally, some concluding remarks are given in section 6.

II. Kinematic Analysis

A. Architecture Description

The schematic diagram of the designed 3-RRPaR translational parallel manipulator is illustrated in Fig. 1. This mechanism consists of a mobile platform, a fixed base, and three limbs of identical RRPaR kinematic structure with the first R joint actuated by a rotary actuator. The notation of R and Pa stands for the revolute joint and parallelogram, respectively.

According to the Fig. 2, for analysis, we assign a fixed frame $O\{x, y, z\}$ at the point O of the fixed base $\Delta A_1A_2A_3$, and a moving frame $P\{u, v, w\}$ at the point P of the mobile platform $\Delta C_1C_2C_3$, with x, y axis parallels to u, v axis, respectively, and the z and w axes perpendicular to the platform. Both the fixed base and moving platform are designed as an isosceles triangle described by the parameter of $r = OA_i$ and $h = PC_i$, respectively, for $i = 1, 2$, and 3. q_{1i} is the actuated variable of the ith limb. B_i denotes the connecting joints between the upper and the lower links. Also, $a=A_iB_i$ and $b=B_iC_i$ are the length of upper and lower links for each limb respectively. Table I describes the optimized architectural parameters of the mechanism.

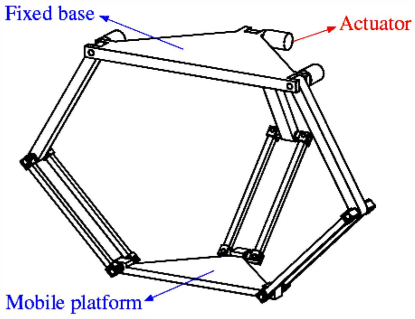

Fig. 1. The designed asymmetrical spatial parallel robot.

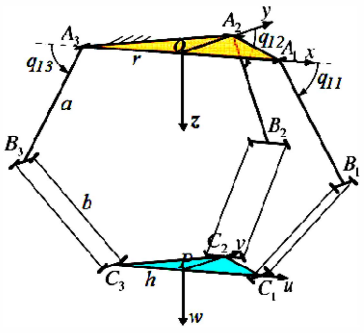

Fig. 2. Schematic representation of a 3-RRPaR parallel manipulator.

TABLE I. Architectural Parameters of the Robot

Parameter	Value	Unit
r	160	mm
a	200	mm
b	200	mm
h	120	mm

B. Inverse Kinematics

In this subsection, the inverse kinematics of suggested parallel manipulator is studied. Figure 3 defines the joint angles associated with the ith limb, wherein p is the point P of the mobile platform position vector. Coordinate system (x_i, y_i, z_i) is attached to the base at point A_i, such that the x_i-axis is in line with the extended line of $\overline{OA}$, the y_i-axis is directed along the revolute joint axis at A_i, and the z_i-axis parallel to the z-axis. The angle $\square_i$, is measured from the x-axis to the x_i-axis and it is a constant parameter in manipulator design. q_{1i} is measured from the x_i-axis to$\overline{AB}$, q_{2i} is defined from the extended line of $\overline{AB}$ to the line defined by the intersection of the plane of the parallelogram and the x_i-z_i plane, and q_{3i} is measured from the y_i direction to $\overline{B_iC_i}$.

A loop-closure equation can be written for each limb:

$$\overline{A_iB_i} + \overline{B_iC_i} = \overline{OP} + \overline{PC_i} - \overline{OA_i} \tag{1}$$

Expressing Eq. 1 in the (x_i, y_i, z_i) coordinate frame, we obtain

$$\begin{bmatrix} acq_{1i} + bsq_{3i}c(q_{1i} + q_{2i}) \\ bcq_{3i} \\ asq_{1i} + bsq_{3i}s(q_{1i} + q_{2i}) \end{bmatrix} = \begin{bmatrix} c_{xi} \\ c_{yi} \\ c_{zi} \end{bmatrix} \tag{2}$$

where

$$\begin{bmatrix} c_{xi} \\ c_{yi} \\ c_{zi} \end{bmatrix} = \begin{bmatrix} c\phi_i & s\phi_i & 0 \\ -s\phi_i & c\phi_i & 0 \\ 0 & 0 & 1 \end{bmatrix} \begin{bmatrix} p_x \\ p_y \\ p_z \end{bmatrix} + \begin{bmatrix} h - r \\ 0 \\ 0 \end{bmatrix} \tag{3}$$

With c stands for cosine, s stands for sine. For inverse kinematic, the position vector p of the mobile platform is given and the problem is to find the joint angles q_{11}, q_{12}, and q_{13} required to bring the mobile platform to the desired position. By solving the second row of Eq. 2, two solutions for q_{3i} are found:

$$q_{3i} = cos^{-1}\frac{c_{yi}}{b} \tag{4}$$

However, it will be shown later that both solutions for q_{3i} result same physical position for limb$i$. After that, q_{2i} can be determined by sum squares of Eq. 2 components.

$$2absq_{3i}cq_{2i} + a^2 + b^2 = c_{xi}^2 + c_{yi}^2 + c_{zi}^2 \tag{5}$$

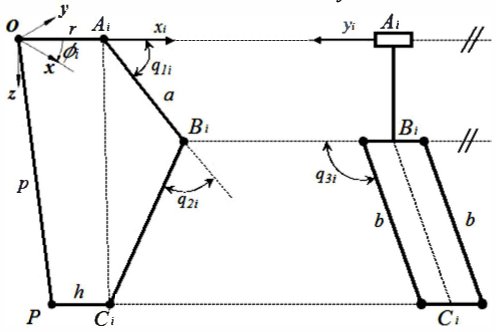

Fig. 3. Description of the joint angles.

Hence

$$q_{2i} = cos^{-1}k \tag{6}$$

where

$$k = (c_{xi}^2 + c_{yi}^2 + c_{zi}^2 - a^2 - b^2)/(2absq_{3i}) \tag{7}$$

Therefore, corresponding to each solution of q_{3i}, Eq. 6 yields two solutions for q_{2i}. These solutions result in four solution sets for q_{2i} and q_{3i}. Furthermore, corresponding to each solution set of q_{2i} and q_{3i}, Eq. 2 yields a unique solution for q_{1i}. However, the four solution sets contain only two distinct values of q_{1i}. Considering these relationships and the limb geometry, each limb assumes the same physical position for each q_{1i}. Hence for each limb four solution sets are realized in only two distinct positions.

C. Jacobian Matrix Generation

Consider $\dot{\mathbf{P}} = [\dot{x} \quad \dot{y} \quad \dot{z}]^T$and $\dot{\mathbf{q}} = [\dot{q}_{11} \quad \dot{q}_{12} \quad \dot{q}_{13}]^T$are the mobile platform output velocities vector and input joint rates vector respectively. The loop-closure in Eq. 1 can be rewritten in to the following form:

$$\overline{OP} + \overline{PC_i} = \overline{OA_i} + \overline{A_iB_i} + \overline{B_iC_i} \tag{8}$$

Differentiating Eq. 8 with respect to time leads to

$$\dot{\mathbf{p}} = \dot{q}_{1i}\mathbf{u}_i \times \mathbf{a}_i + \omega_{bi} \times \mathbf{b}_i \tag{9}$$

where ω_{bi} denotes the angular velocity of the ith lower link, $\mathbf{a}_i = \overline{A_iB_i}$, $\mathbf{b}_i = \overline{B_iC_i}$, and

$$\mathbf{u} = \left[c(\frac{\pi}{2} + \phi_i) \quad s(\frac{\pi}{2} + \phi_i) \quad 0\right]^T \tag{10}$$

with $\phi_i = \frac{\pi}{2}(i-1)$, for i=1, 2, and 3. To eliminate the passive joint rate ω_{bi}, we dot-multiply both sides of Eq. 10 by $\mathbf{b}_i$. This leads to

$$\mathbf{b}_i{}^T\dot{\mathbf{p}} = \dot{q}_{1i}\mathbf{u}_i{}^T.(\mathbf{a}_i \times \mathbf{b}_i) \tag{11}$$

Writing Eq. 11 three times, for i =1, 2, and 3, it yields three scalar equations into a matrix form as follows:

$$\mathbf{A}\dot{\mathbf{p}} = \mathbf{B}\dot{\mathbf{q}} \tag{12}$$

Where

$$\mathbf{A} = \begin{bmatrix} \mathbf{b}_1^{\mathrm{T}} \\ \mathbf{b}_2^{\mathrm{T}} \\ \mathbf{b}_3^{\mathrm{T}} \end{bmatrix}, \quad \mathbf{B} = \begin{bmatrix} \mathbf{u}_1{}^{\mathrm{T}}.(\mathbf{a}_1 \times \mathbf{b}_1) \\ \mathbf{u}_2{}^{\mathrm{T}}.(\mathbf{a}_2 \times \mathbf{b}_2) \\ \mathbf{u}_3{}^{\mathrm{T}}.(\mathbf{a}_3 \times \mathbf{b}_3) \end{bmatrix} \tag{13}$$

In view of Eq. 12, we can relate output velocities to the actuated joint velocities when the parallel mechanism is away from singularities

$$\dot{\mathbf{q}} = \mathbf{J}\dot{\mathbf{p}} \tag{14}$$

Where $\mathbf{J}$=$\mathbf{B}^{-1}\mathbf{A}$, and $\mathbf{J} \in \mathbb{R}^{3\times3}$represents the Jacobian matrix of the robot.

III. DYNAMIC ANALYSIS

In this section, we will perform the inverse dynamic modeling of the parallel manipulator based upon the principle of virtual work. The inverse dynamics problem is to find the actuator torques and/or forces required to generate a desired trajectory of the manipulator.

A. Simplification Hypothesis

Without losing generality of model, we can simplify the dynamic problem by the following hypotheses:

The connecting rods of lower links can be built with light materials such as the aluminum alloy, so

- The lower links rotational inertias are neglected;
- The mass of each lower links, is divided evenly and concentrated at the two endpoints B_i and C_i.

Also it is supposed that:

- The friction forces in joints are neglected.
- No external forces suffered.

B. Dynamic Modeling

We consider that $\boldsymbol{\tau} = [\tau_1 \quad \tau_2 \quad \tau_3]^T$and $\delta\mathbf{q} = [\delta q_{11} \quad \delta q_{12} \quad \delta q_{13}]^T$are the vector of actuator torques and vector of corresponding virtual angular displacements. Furthermore, $\delta\mathbf{p} = [\delta x \quad \delta y \quad \delta z]^T$represents the virtual linear displacements vector of the mobile platform. Dynamic parameters of the manipulator are described in Table II. We can derive the following equations by applying the virtual work principle.

$$\boldsymbol{\tau}^T\delta\mathbf{q} + \mathbf{M}_{Ga}^T\delta\mathbf{q} + \mathbf{F}_{Gp}^T\delta\mathbf{p} - \mathbf{M}_a^T\delta\mathbf{q} - \mathbf{F}_p^T\delta\mathbf{p} = 0 \tag{15}$$

Where

$$\mathbf{M}_{Ga} = \left(\frac{1}{2}m_a + m_b\right)ga\mathbf{I}[cq_{11} \quad cq_{12} \quad cq_{13}]^T \tag{16}$$

is the upper links gravity torques vector. m_a and m_b are mass of upper link and each connecting rod of lower link, respectively. Here g denotes the gravity acceleration, and $\mathbf{I}$ represents the 3×3 identity matrix.

$$\mathbf{F}_{Gp} = [0 \quad 0 \quad -(m_p + 3m_b)g]^T \tag{17}$$

denotes the mobile platform gravity force vector, and m_p is mass of the mobile platform.

$$\mathbf{M}_a = \hat{\mathbf{I}}_a\ddot{\mathbf{q}} = \hat{\mathbf{I}}_a[\ddot{q}_{11} \quad \ddot{q}_{12} \quad \ddot{q}_{13}]^T \tag{18}$$

represents the upper links inertia torques vector and $\hat{\mathbf{I}}_a = \left(\frac{1}{3}m_aa^2 + m_ba^2\right)\mathbf{I}$ denotes the upper links inertial matrix with respect to the fixed frame $O\{x, y, z\}$, and

$$\mathbf{F}_p = \hat{\mathbf{M}}_p\ddot{\mathbf{p}} = \left(m_p + 3m_b\right)\mathbf{I}[\ddot{x} \quad \ddot{y} \quad \ddot{z}]^T \tag{19}$$

denotes the mobile platform inertial forces vector. Equation 14, can be written into the following form

$$\dot{\mathbf{p}} = \mathbf{J}^{-1}\dot{\mathbf{q}} \tag{20}$$

Consequently,

$$\delta\mathbf{p} = \mathbf{J}^{-1}\delta\mathbf{q} \tag{21}$$

Substituting Eq. 21 into Eq. 15, results

$$(\boldsymbol{\tau}^T + \mathbf{M}_{Ga}^T + \mathbf{F}_{Gp}^T\mathbf{J}^{-1} - \mathbf{M}_a^T - \mathbf{F}_p^T\mathbf{J}^{-1})\delta\mathbf{q} = 0 \tag{22}$$

Equation 22 holds for any virtual displacements δq, so we have

$$\boldsymbol{\tau} = \mathbf{M}_a + \mathbf{J}^{-T}\mathbf{F}_p - \mathbf{M}_{Ga} - \mathbf{J}^{-T}\mathbf{F}_{Gp} \tag{23}$$

Substituting Eqs. 18 and 19 into Eq. 23, allows the generation of

$$\boldsymbol{\tau} = \hat{\mathbf{I}}_a\ddot{\mathbf{q}} + \mathbf{J}^{-T}\hat{\mathbf{M}}_p\ddot{\mathbf{p}} - \mathbf{M}_{Ga} - \mathbf{J}^{-T}\mathbf{F}_{Gp} \tag{24}$$

TABLE II. DYNAMIC PARAMETERS OF THE ROBOT

Parameter	Value	Unit
m_p	0.4	Kg
m_a	0.3	Kg
m_b	0.1	Kg
g	9.8	m/s²

Differentiating Eq. 20 with respect to time, yields

$$\ddot{\mathbf{p}} = \mathbf{J}^{-1}\ddot{\mathbf{q}} + \dot{\mathbf{J}}^{-1}\dot{\mathbf{q}} \tag{25}$$

Substituting Eq. 25 into Eq. 24, we can derive that

$$\boldsymbol{\tau} = \mathbf{M}(\mathbf{q})\ddot{\mathbf{q}} + \mathbf{C}(\mathbf{q},\dot{\mathbf{q}})\dot{\mathbf{q}} + \mathbf{G}(\mathbf{q}) \tag{26}$$

Equation 26 represents the dynamic model of parallel manipulator in joint space. Here, $\mathrm{q} \in \mathbb{R}^3$ is the controlled variables, and

$$\mathbf{M}(\mathbf{q}) = \hat{\mathbf{I}}_a + \mathbf{J}^{-T}\hat{\mathbf{M}}_p\mathbf{J}^{-1}$$

Denotes a symmetric positive definite inertial matrix, that $\mathbf{M}(\mathbf{q}) \in \mathbb{R}^{3\times3}$.

$$\mathbf{C}(\mathbf{q},\dot{\mathbf{q}}) = \mathbf{J}^{-T}\hat{\mathbf{M}}_p\dot{\mathbf{J}}^{-1}$$

Where $\mathbf{C}(\mathbf{q},\dot{\mathbf{q}}) \in \mathbb{R}^{3\times3}$ is the centrifugal and Coriolis forces matrix, and

$$\mathbf{G}(\mathbf{q}) = -\mathbf{M}_{Ga} - \mathbf{J}^{-T}\mathbf{F}_{Gp}$$

represents the vector of gravity forces, and $\mathbf{G}(\mathbf{q}) \in \mathbb{R}^3$.

IV. The Control System Structure

A. Computed Torque Control via PD and PID Controller

In this section, we implement the computed torque control (C-T) method in joint space for considered parallel manipulator. This approach is commonly used in the robotics control systems and able to make the error asymptotically stable [24].

Equation 26 can be rewritten as:

$$\boldsymbol{\tau} = \mathbf{M}(\mathbf{q})\ddot{\mathbf{q}} + \mathbf{H}(\mathbf{q},\dot{\mathbf{q}}) \tag{27}$$

where $\mathbf{H}(\mathbf{q},\dot{\mathbf{q}}) = \mathbf{C}(\mathbf{q},\dot{\mathbf{q}})\dot{\mathbf{q}} + \mathbf{G}(\dot{\mathbf{q}})$.

Block diagram of the C-T control system implemented with conventional PD and PID feedback is shown in Fig. 4. By the following joint torques the parallel robot can be actuated.

$$\boldsymbol{\tau} = \hat{\mathbf{M}}(\mathbf{q})\mathbf{u} + \hat{\mathbf{H}}(\mathbf{q},\dot{\mathbf{q}}) \tag{28}$$

Where in Eq. 28, $\hat{\mathbf{M}}(\mathbf{q})$ and $\hat{\mathbf{H}}(\mathbf{q}, \dot{\mathbf{q}})$denotes the estimation of $\mathbf{M}(\mathbf{q})$ and $\mathbf{H}(\mathbf{q}, \dot{\mathbf{q}})$ respectively, and $\mathbf{u}$ is an input signal in acceleration form. Combining Eqs. 27 and 28, it yields a linear second order system as follows

$$\ddot{\mathbf{q}} = \mathbf{u} \tag{29}$$

There are many possible choices for perfect tracking in a PD [25], and PID feedback implementation:

$$\mathbf{r} = \ddot{\mathbf{q}}_d + \mathbf{K}_D\dot{\mathbf{q}}_d + \mathbf{K}_P\mathbf{q}_d \tag{30}$$

$$\mathbf{r} = \ddot{\mathbf{q}}_d + \mathbf{K}_D\dot{\mathbf{q}}_d + \mathbf{K}_I\int_0^t \mathbf{q}_d\,d(t) + \mathbf{K}_P\mathbf{q}_d \tag{31}$$

where in Eqs. 30 and 31, $\mathbf{r}$ denotes the reference signal for PD and PID feedback implementation respectively, $\mathbf{K}_P$, $\mathbf{K}_I$ and $\mathbf{K}_D$ denote the conventional PID gains matrices, and $\mathbf{q}_d$ denotes the desired joint trajectory.

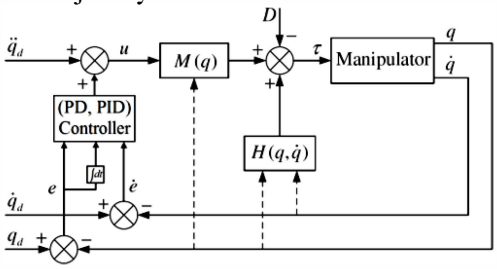

Fig. 4. Block diagram of C-T control with PD and PID.

Then the acceleration input signal in Eq. 29 can be rewritten in to the following form:

$$\mathbf{u} = \mathbf{r} - \mathbf{K}_D\dot{\mathbf{q}} - \mathbf{K}_P\mathbf{q} = \ddot{\mathbf{q}}_d + \mathbf{K}_D(\dot{\mathbf{q}}_d - \dot{\mathbf{q}}) + \mathbf{K}_P(\mathbf{q}_d - \mathbf{q}) \tag{32}$$

$$\mathbf{u} = \mathbf{r} - \mathbf{K}_D\dot{\mathbf{q}} - \mathbf{K}_I\int_0^t \mathbf{q}d(t) - \mathbf{K}_P\mathbf{q}$$

$$= \ddot{\mathbf{q}}_d + \mathbf{K}_D(\dot{\mathbf{q}}_d - \dot{\mathbf{q}}) + \mathbf{K}_I\int_0^t (\mathbf{q}_d - \mathbf{q})d(t) + \mathbf{K}_P(\mathbf{q}_d - \mathbf{q}) \tag{33}$$

Substituting Eqs. 32 and 33into Eq. 29, result the equations of error 34 and 35 respectively:

$$\ddot{\mathbf{e}} + \mathbf{K}_D\dot{\mathbf{e}} + \mathbf{K}_P\mathbf{e} = 0 \tag{34}$$

$$\ddot{\mathbf{e}} + \mathbf{K}_D\dot{\mathbf{e}} + \mathbf{K}_I\int_0^t \mathbf{e}d(t) + \mathbf{K}_P\mathbf{e} = 0 \tag{35}$$

By specifying suitable values of feedback gains $\mathbf{K}_P$, $\mathbf{K}_I$ and $\mathbf{K}_D$, trajectory tracking error will go to zero asymptotically.

B. Computed Torque Control via Fuzzy Supervisory Control

Figure 5 represents the general architecture of a two-level fuzzy control system, where the first level is a conventional controller and the second level consists of fuzzy systems that supervise and modify the operations of the conventional controller. Block diagram of the C-T control system implemented with fuzzy PD and PID controller is illustrated in Fig. 6. In this design, the inference mechanism of fuzzy logic includes a two-input–single-output component and we use two-dimensional linear rule base as the mapping of the input linguistic variables error $e(t)$ and error derivative $\dot{e}(t)$ onto the fuzzy logic output linguistic variable (u_{fuzzy}). To judge the performance quality of the control systems, various performance criteria exist. Here, in order to tune the PD and PID parameters, the performance criterion Integral of Absolute Error (IAE) has been utilized, because it could weight latest-errors.

$$\mathrm{IAE} = \int_0^t \left| y_{des}(t) - y_{act}(t) \right| dt = \int_0^t |e(t)|\,dt \tag{36}$$

Where y_{des} is the desired trajectory, i.e., desired joint angular displacements, and y_{act} is the actual response, i.e., actual joint angular displacements. We employ standard triangular membership functions and Mamdani type inference engine by using center of gravity method defuzzification for fuzzy logic output (u_{fuzzy}). Table 3 shows design of the fuzzy rules, which the range of the error $e(t)$ and error derivative $\dot{e}(t)$ are divided into seven partitions. In Table III, the linguistic variables (NB), (NM), (NS), (ZO), (PS), (PM), (PB) represent negative big, negative medium, negative small, zero, positive small, positive medium and positive big respectively.

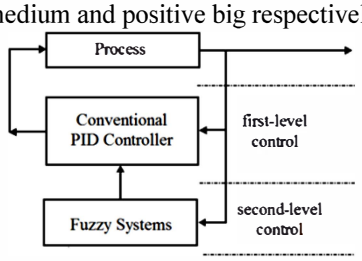

Fig. 5. Architecture of a two-level fuzzy control system.

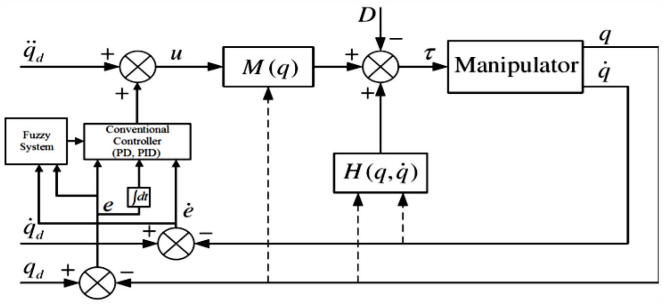

Fig. 6. Block diagram of C-T control with Fuzzy supervisory control.

V. Simulation Results

A complex described trajectory of mobile platform in the Cartesian space is considered for simulation studies in order to investigate the obtained kinematic and dynamic model.

$$x = -0.1\sin(\pi t)$$
$$y = 0.1\cos(\pi t) \qquad (37)$$
$$z = -0.29 + 0.05\cos\left(\frac{\pi}{2}t\right)$$

Where t denotes the time variable, and x, y and z are in units of meters. According to the parameters of Table I and II, the simulation results of kinematic and dynamic model are shown in Fig. 7, where Fig. 7(a) to 7(c) illustrate the joint angular displacements, velocities, and accelerations, respectively, which are derived via closed-form solutions of inverse kinematic. And Fig. 7(d) demonstrates the actuated joint torques, which generated by inverse dynamic model of manipulator.

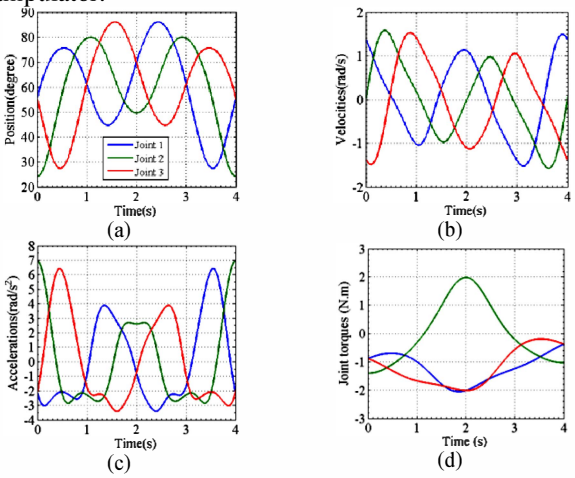

Fig. 7. Simulation results for joint angular (a) displacements, (b) velocities, (c) accelerations, and (d) joint torques.

TABLE III. Rule-table of the Fuzzy-PID

e / $\dot{e}$	*NB*	*NM*	*NS*	*ZO*	*PS*	*PM*	*PB*
PB	ZO	PS	PM	PB	PB	PB	PB
PM	NS	ZO	PS	PM	PB	PB	PB
PS	NM	NS	ZO	PS	PM	PB	PB
ZO	NB	NM	NS	ZO	PS	PM	PB
NS	NB	NB	NM	NS	ZO	PS	PM
NM	NB	NB	NB	NM	NS	ZO	PS
NB	NB	NB	NB	NB	NM	NS	ZO

Figure 8 shows the simulation results in order to compare the ability of tracking in the presence of disturbance for various methods which are designed in previous section. Assuming that disturbance D = 1 N.m in the form of external torque has been exerted to the mobile platform at t = 1.15 sec. Figure 8(a) to 8(d) represent the trajectory tracking of C-T method implemented with PD, PID, Fuzzy-PD and Fuzzy-PID supervisory control, respectively. It is observed that all of these applied methods cause the joint space error asymptotically converges to zero, but according to the IAE criterion, which is given in detail in Table IV, it can be clearly seen that the fuzzy supervisory approach shows superior performance than its corresponding conventional controller due to its gain scheduling capability when the robot is exposed in the disturbance condition. Figure 9 illustrates this appealing characteristic, e.g., for joint 3, where Fig. 9(a) to 9(c) describe the readjustment of PID gains via fuzzy system as a master controller.

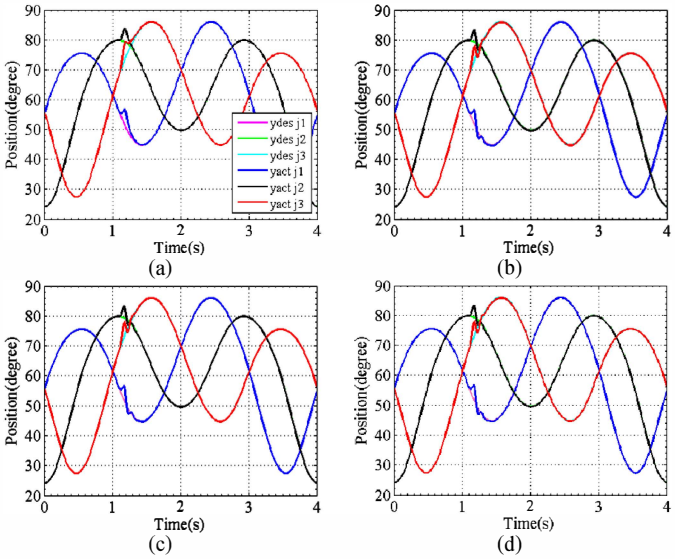

Fig. 8. Simulation results of trajectory tracking for C-T method with (a) PD, (b) PID, (c) Fuzzy-PD, and (d) Fuzzy-PID supervisory control.

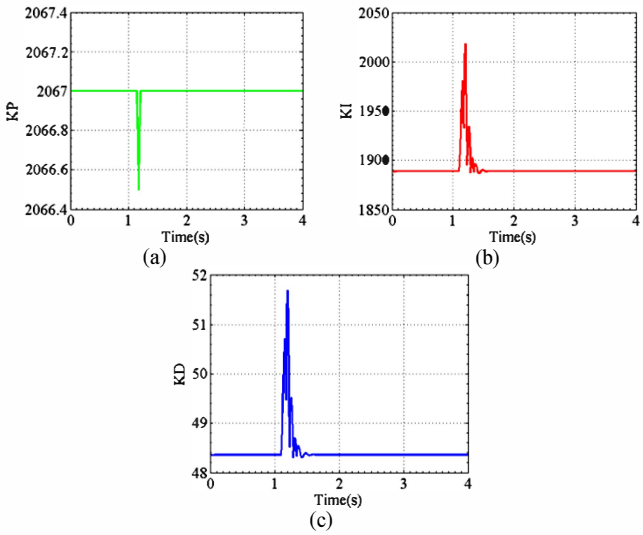

Fig. 9. Readjustment of (a) K_P, (b) K_I, and (c) K_D with Fuzzy-PID supervisory control.

TABLE IV. JOINT TRACKING ERRORS

Without Disturbance					In the Presence of Disturbance				
Joint Number	***PD***	***PID***	***Fuzzy PD***	***Fuzzy PID***	***PD***	***PID***	***Fuzzy PD***	***Fuzzy PID***	***Unit***
1	0.0487	0.0089	0.0485	0.0080	0.9494	0.8562	0.5925	0.4525	*rad*
2	0.0484	0.0078	0.0481	0.0068	0.7993	0.7165	0.4982	0.4161	*rad*
3	0.0501	0.0082	0.0498	0.0073	0.9695	0.8650	0.5975	0.5604	*rad*
IAE	0.1472	0.0249	0.1464	0.0221	2.7182	2.4377	1.6881	1.4290	*rad*

VI. CONCLUSIONS

In this study, a new structure of spatial parallel manipulator with three degrees of pure translational freedom from DELTA robots family was presented. At first, the inverse kinematic model of robot has been carried out. For inverse kinematic problem, these solutions demonstrate that, in general, there are two possible poses for each limb. After that the Jacobian matrix was derived analytically. Then by employing the principle of virtual work, inverse dynamic model has been established. For improving efficiency and accuracy of conventional PID controller, when dynamic of robot strongly is affected by nonlinearity and disturbances, the supervisory control has been employed to re-adjust the PID gains. So, effect of disturbance in the parallel manipulator has been handled in this paper by using supervisory control system. The lower level is a conventional PD and PID controller, which controls the parallel manipulators to the desired trajectory. The upper-level supervisory controller consists of fuzzy logic controller for scheduling the PID gains. By minimizing IAE as a performance criterion, we have also compared this new C-T methodology, which implemented by supervisory controller, with another closely related and comparable C-T method in simulation. Simulation results indicate that proposed method is better than the common C-T method with conventional controller in trajectory tracking and especially adapting itself to disturbance conditions. It should be noted that the robotic system with disturbance problems evidently contains common problems, as a special class. Therefore, the proposed control methodology is extensively applicable to control of any robotic systems.

REFERENCES

[1] Y Lu, S Li, C Du, J Yu, J Xu, "Simulation of normal machining of 3D free-form surface by an orthogonal 3-leg parallel machine tool with 5-DOF," *Computers & Industrial Engineering*, vol. 59, pp. 764 – 769, 2010.

[2] PK Jamwal, SQ Xie, YH Tsoi, KC Aw, "Forward kinematics modelling of a parallel ankle rehabilitation robot using modified fuzzy inference," *Mechanism and Machine Theory*, vol. 45, pp. 1537 – 1554, 2010.

[3] W. Khalil, O. Ibrahim, "General solution for the dynamic modeling of parallel robots,"*Journal of Intelligent and Robotic Systems*, vol. 49, pp. 19–37, 2007.

[4] Staicu, S., Liu, X.-J., Wang, J., "Inverse dynamics of the HALF parallel manipulator with revolute actuators," *Nonlinear Dy.*, vol. 50, pp. 1–12, 2007.

[5] Staicu, S., Zhang, D., "A novel dynamic modeling approach for parallel mechanisms analysis,"*Robot. Comput.-Integr. Manuf.*, vol. 24, pp. 167–172, 2008.

[6] Staicu, S., "Recursive modeling in dynamics of Agile Wrist spherical parallel robot," *Robot. Comput.-Integr. Manuf.*, vol. 25, pp. 409–416, 2009.

[7] Li, Y., Xu, Q., "Kinematics and Inverse Dynamics Analysis for a General 3-PRS Spatial Parallel Mechanism," *Robotica*, vol. 23, pp. 219-229, 2005.

[8] H.A. Malki, D.Misir, D. Feigenspan, G. Chen, "Fuzzy PID control of a flexible-joint robot-arm with uncertainties from time-varying loads,"*IEEE Trans, on Cont. Syst. Tech.*, vol. 5, pp. 371-378, 1997.

[9] Y.-T. Juang, Y.-T. Chang, C.-P. Huang, "Design of fuzzy PID controllers using modified triangular membership functions,"*Information Sciences*,vol. 178, pp. 1325–1333, 2008.

[10] Mohan BM, SinhaArpita, "Mathematical models of the simplest fuzzy PI/PD controllers with skewed input and output fuzzy sets,"*ISA Transactions*, vol. 47, pp. 300–310, 2008.

[11] Fadaei A, SalahshoorK., "Design and implementation of a new fuzzy PID controller for networked control systems,"*ISA Transactions*, vol. 47, pp. 351–361, 2008.

[12] Li Han-Xiong, Zhang Lei, Cai Kai-Yuan, Chen Guanrong,"An improved robust fuzzy PID controller with optimal fuzzy reasoning," *IEEE Transactions on Systems, Man and Cybernetics, Part B (Cybernetics)*, vol. 35, pp. 1283–1294, 2005.

[13] Kazemian Hassan B., "Comparative study of a learning fuzzy PID controller anda self-tuning controller,"*ISA Transactions*, vol. 40, pp. 245–253, 2001.

[14] H. Ying, W. Siler, J.J. Buckley, "Fuzzy control theory: Anonlinear case,"*Automatica*,vol. 26, pp. 513-520, 1990.

[15] G. Chen, "Conventional and fuzzy PID controllers: An overview," *Int. J. Intell. Cont. Syst.*, vol. 1, pp. 235-246, 1996.

[16] MudiRajani K, Pal Nikhil R.,"A robust self-tuning scheme for PI-and PD-type fuzzy controllers,"*IEEE Transactions on Fuzzy Systems*, vol. 7, pp. 2–16, 1999.

[17] MudiRajani K., Pal Nikhil R., "A self-tuning fuzzy PI controller,"*Fuzzy Sets andSyst.*, vol. 115, pp. 327–338, 2000.

[18] Bhattacharya S, Chatterjee A, Munshi S.,"A new self tuned PID-type fuzzycontroller as a combination of two-term controllers,"*ISA Transactions*, vol. 43, pp. 413–426, 2004.

[19] Mohsen Asgari and Mahdi. A. Ardestani, "Advanced Dynamic Path Control of a 3-DOF Spatial Parallel Robot using Adaptive Neuro Fuzzy Inference System," *18th annual Conference on Mechatronics and Machine Vision in Practice, Brisbane, 2011*.

[20] J.-S. Chiou, M.-T. Liu, "Numerical simulation for fuzzy-PID controllers and helping EP reproduction with PSO hybrid algorithm," *Simulation Modelling Practice and Theory*, vol. 17, pp. 1555–1565, 2009.

[21] Boubertakh Hamid, Tadjine Mohamed, Glorennec Pierre-Yves, "Tuning fuzzy PD and PI controllers using reinforcement learning,"*ISA Transactions*, vol. 49, pp. 543–551, 2010.

[22] Mohan BM, SinhaArpita., "Analytical structure and stability analysis of a fuzzyPID controller,"*Applied Soft Computing*, vol. 8, pp. 749–758, 2008.

[23] G. Chen, H. Ying, "BIBIO stability of nonlinear fuzzy PI control system," *J. Intell. Fuzzy Syst*. Vol. 5, pp. 245-256, 1997.

[24] Prabu,D., Kumar,S., Prasad, R., "Dynamic Control of Three-Link SCARA Manipulator using Adaptive Neuro Fuzzy Inference System,"*IEEE International Conference on Networking, Sensing and Control*, 2008.

[25] J. J. Craig, *Introduction to Robotics: Mechanics and Control*, 3rd ed.Reading, MA: Addison-Wesley, 2009.